

1
2
3
4
5
6
7
8
9
10
11
12
13
14
15
16
17

**RECOVERY OF 150-250 MeV/nuc COSMIC RAY HELIUM NUCLEI
INTENSITIES BETWEEN 2004-2010 NEAR THE EARTH,
AT VOYAGER 2 AND AT VOYAGER 1 IN THE HELIOSHEATH
– A TWO ZONE HELIOSPHERE**

W.R Webber¹, F.B. McDonald², P.R. Higbie³ and B. Heikkila⁴

1. New Mexico State University, Department of Astronomy, Las Cruces, NM, 88003, USA
2. University of Maryland, Institute of Physical Science and Technology, College Park, MD, 20742, USA
3. New Mexico State University, Physics Department, Las Cruces, NM, 88003, USA
4. NASA/Goddard Space Flight Center, Greenbelt, MD 20771, USA

18
19
20
21
22
23
24
25
26
27
28
29
30
31
32
33
34
35
36
37
38
39
40
41

Abstract

The recovery of cosmic ray He nuclei of energy $\sim 150\text{-}250$ MeV/nuc in solar cycle #23 from 2004 to 2010 has been followed at the Earth using IMP and ACE data and at V2 between 74-92 AU and also at V1 beyond the heliospheric termination shock (91-113 AU). The correlation coefficient between the intensities at the Earth and at V1 during this time period is remarkable (0.921), after allowing for a ~ 0.9 year delay due to the solar wind propagation time from the Earth to the outer heliosphere. The intensity measured at V1 is ~ 6 times that at the Earth in 2005 at the beginning of the recovery but at 2010.5 this difference is only a factor ~ 2.2 as a result of the fact that the relative intensity increase at the Earth is larger than that at V1. To describe these intensity changes and to predict the absolute intensities measured at all three locations we have used a simple spherically symmetric (no drift) two-zone heliospheric transport model with specific values for the diffusion coefficient in both the inner and outer zones. The diffusion coefficient in the outer zone, assumed to be the heliosheath from about 90 to 120 (130) AU, is determined to be ~ 5 times smaller than that in the inner zone out to 90 AU. This means the Heliosheath acts much like a diffusing barrier in this model. The absolute magnitude of the intensities and the intensity changes at V1 and the Earth are described to within a few percent by a diffusion coefficient that varies with time by a factor ~ 4 in the inner zone and only a factor of ~ 1.5 in the outer zone over the time period from 2004-2010. For V2 the observed intensities follow a curve that is as much as 25% higher than the calculated intensities at the V2 radius and at times the observed V2 intensities are equal to those at V1. At least one-half of the difference between the calculated and observed intensities between V1 and V2 can be explained if the heliosphere is squashed by $\sim 10\%$ in distance (non-spherical) so that the HTS location is closer to the Sun in the direction of V2 compared to V1.

42 **Introduction**

43 The intensity recovery of galactic cosmic rays at the Earth in the current solar 11-year cycle
44 between 2004-2009 is well documented using spacecraft data (e.g., McDonald, Webber and
45 Reames, 2010; Mewaldt, et al., 2009, 2010). This cosmic ray recovery started in early 2004 at
46 the Earth after the large “Halloween” events in October-November, 2003, and has been observed
47 by neutron monitors and various spacecraft near the Earth including ACE, IMP and others. This
48 recovery was observed by V2 and V1 to begin in the outer heliosphere in late 2004 after the
49 Halloween event had propagated out to their respective locations at 76 and 93 AU (McDonald, et
50 al., 2006). At the end of 2004 V1 crossed the Heliospheric Termination Shock (HTS) at 94 AU
51 and has continued to move outward so that by 2010.5 it was at ~114 AU, perhaps ~30 AU or
52 more beyond the current HTS location, estimated to be between 80-85 AU (Webber, 2011).
53 Thus V1 has spent essentially the entire recovery cycle beyond the HTS in the heliosheath region
54 where the solar wind parameters are measurably different from those in the inner heliosphere.
55 V2 remained in the “inner” part of the heliosphere, ~15 AU closer to the sun until 2007.66 when
56 at a distance of ~84 AU it also crossed the HTS.

57 At about 2010.0 the cosmic ray Helium nuclei intensity at the Earth reached its maximum.
58 At V1 the intensity continues to increase as of 2010.5 whereas at V2 it reached a maximum in
59 early 2009. At the Earth the intensities reached levels ~25% higher than those observed during
60 the previous 11-year intensity maximum in 1997-98 (McDonald, Webber and Reames, 2010;
61 Mewaldt, et al., 2009, 2010). At V1 the cosmic ray Helium intensities are at the highest levels
62 yet observed in the heliosphere and at energies ~200 MeV/nuc at 2010.5 are within ~10-20% of
63 the estimated LIS intensity for Helium nuclei at this energy (see Webber and Higbie, 2009).

64 It is the purpose of this paper to compare the Helium intensities between 150-250
65 MeV/nuc observed at the Earth and those observed at V1 and V2 during this extended time
66 period within the framework of a simple modulation model, with the objective of understanding
67 better the global characteristics of the solar 11-year modulation cycle, including particularly the
68 modulation effects beyond the HTS in the heliosheath.

69 We anticipate that this is the first of several articles dealing with the recovery of cosmic
70 ray intensities at V1, V2 and the Earth during this extended time period. Other articles will
71 include 150-250 MeV protons and 20-125 MeV/nuc Carbon nuclei also measured at these

72 locations during this time period. Each type of particle gives its own specific information about
73 the heliosphere modulation process and the required “source” spectrum of the particles involved.

74 **Observations at the Earth and at V1 and V2**

75 In Figure 1 we show the time history of $\sim 130\text{-}250$ MeV/nuc He nuclei at the Earth from
76 2004 to the present time. This data is smoothed by taking 5 times 26 day moving averages. The
77 data at the Earth is a composite of IMP and ACE data as constructed by McDonald, Webber and
78 Reames, 2010. Also shown in this Figure are the corresponding intensities for $\sim 155\text{-}245$
79 MeV/nuc He nuclei at V1 and V2 corrected for a background of low energy ACR He ($\sim 10\%$ or
80 less at these energies). At the beginning of the recovery time period the intensity at V1 was ~ 6
81 times that at the Earth. This is a measure of the overall interplanetary gradient between 1 and
82 ~ 94 AU, the location of V1 at that time. By 2010.5 this intensity ratio is reduced to ~ 2.2
83 implying that the intensity changes between 2004 and 2010.5 at the Earth are much greater than
84 those at V1. This changing intensity ratio is shown in Figure 2. In Figure 3 we show the data at
85 the Earth superimposed on the data at V1 (with different intensity scales), with the data at Earth
86 delayed to account for the solar wind propagation time from the Earth to V1. This delay time is
87 varied from 0.5 to 1.5 years in 26 day increments and the correlation coefficient reaches a
88 maximum value 0.922 for time delays between 0.86 and 0.93 years. This correspondence of
89 time histories is remarkable considering the ~ 100 AU difference in the radial location of the
90 spacecraft.

91 This correlation throughout the heliosphere is also evident in Figure 4A which shows the
92 intensities at V1 and V2 vs. those at the Earth, with a delay ~ 0.89 yrs. The “loop” in the
93 regression curves between V1 and V2 and the Earth data in Figure 4A is due to the largest
94 transient cosmic ray decrease in solar cycle #23 (the September, 2005, event at the Earth)
95 propagating outward through the heliosphere, reaching V2 at ~ 2006.15 and V1 at about 2006.5.
96 If this time period is excluded from the correlation calculation, the maximum value for the
97 correlation coefficient between V1 and the Earth intensities increases to 0.961 for a delay of 0.89
98 years.

99 We seek to fit the data in Figure 4A and to interpret it using a simple global modulation
100 model. This model should predict the absolute intensities at all three locations and also the
101 changing ratios of intensities at V1 beyond the HTS, at V2 mainly just inside the HTS, and those
102 intensities at the Earth vs. time as given by Figure 2 and also Figure 4A. In addition the slopes

103 of the regression lines between V1 and V2 and the Earth, that is the ratio of the rates of change
 104 of intensity at each location needs to be fit. A simple inspection of Figures 1 and 4A shows that
 105 the intensity changes at the Earth are much larger than those at V1 or V2 even though the particle
 106 energies are nearly the same.

107 From Figure 1 we observe that the He intensities at V2 were nearly the same as those at
 108 V1 during the minimum modulation period from 1998 to the middle of 2000. Then with
 109 increased modulation a sustained radial gradient was established between the two spacecraft
 110 which continued until after the large transient decrease in 2006 noted above, passed V2 and then
 111 V1. From early 2007 to early in 2009 the intensities at both spacecraft were almost identical
 112 again. Early in 2009 the intensity at V2 stopped increasing and by 2010.5 the difference in V1
 113 and V2 intensities was ~20% implying again a sustained radial gradient between the two
 114 spacecraft.

115 **The Cosmic Ray Transport Equation in the Heliosphere**

116 Here we use a simple spherically symmetric quasisteady state no-drift transport model for
 117 cosmic rays in the heliosphere. While this simplified model obviously cannot fit all types of
 118 observations it does provide a useful insight into the inner heliospheric/outer heliospheric
 119 modulation and helps to determine which aspects of this modulation need more sophisticated
 120 models for their explanation such as a recent multi-dimensional model by Florinski and
 121 Pogorelev, 2009. The numerical model was originally provided to us by Moraal (2003) and is
 122 similar to the model described originally in Reinecke, Moraal and McDonald, 1993, and in
 123 Caballero-Lopez and Moraal (2004), and also to the spherically symmetric transport model
 124 described by Jokipii, Kota and Merenyi, 1993 (Figure 3 of that paper). The basic cosmic ray
 125 transport equation used is (Gleeson and Urch, 1971);

$$126 \quad \frac{\partial f}{\partial t} + \nabla \cdot (CVf - K \cdot \nabla f) + \frac{1}{3p^2} \frac{\partial}{\partial p} (p^2 V \cdot \nabla f) = Q$$

127 Here f is the cosmic ray distribution function, p is momentum, V is the solar wind velocity,
 128 $K(r,p,t)$ is the diffusion tensor, Q is a source term and C is the so called Compton-Getting
 129 coefficient.

130 For spherical symmetry (and considering latitude effects to be unimportant for this
 131 calculation) the diffusion tensor becomes a single radial coefficient K_{rr} . We assume that this
 132 coefficient is separable in the form $K_{rr}(r,P) = \beta K_1(P) K_2(r)$, where the rigidity part, $K_1(P) \equiv K_1$

133 and radial part, $K_2(r) \equiv K_2$. The rigidity dependence of $K(P)$ is assumed to be $\sim P$ above a low
 134 rigidity limit P_B . The units of the coefficient K_{rr} are in terms of the solar wind speed $V=4 \cdot 10^2$
 135 $\text{km}\cdot\text{s}^{-1}$, and distance in $\text{AU} = 1.5 \cdot 10^8 \text{ km}$, so $K_{rr} = 6 \cdot 10^{20} \text{ cm}^2 \cdot \text{s}^{-1}$ when $K_1 = 1.0$.

136 We consider two possible scenarios. The first is a simple heliosphere with the diffusion
 137 coefficient varying out to some outer boundary r , here taken to be 120 (130) AU, and the solar
 138 wind speed V , = const = $400 \text{ km}\cdot\text{s}^{-1}$. This is a one zone heliosphere first described by Parker,
 139 1965. The second scenario is a two zone heliosphere (e.g., Jokipii, Kota and Merenyi, 1993). In
 140 this case the inner zone extends out to 90 AU, the average distance to the HTS. In this inner
 141 region $V=400 \text{ km}\cdot\text{s}^{-1}$ and the diffusion parameters K_1 and K_2 are determined in our approach by
 142 a fit to the cosmic ray data being compared (the Earth and V2) rather than using e.g., consensus
 143 values (Palmer, 1982) appropriate to the “local” heliosphere.

144 The outer zone extends from 90 AU to ~ 120 (130) AU, the approximate distance to the
 145 heliopause (HP) or an equivalent “outer boundary” and essentially encompasses the heliosheath.
 146 In this region V is taken to be $130 \text{ km}\cdot\text{s}^{-1}$ (from V2 measurements, Richardson, et al., 2008) and
 147 the diffusion parameters are K_{1H} and K_{2H} , which are different from those in the inner
 148 heliosphere, and again determined by the cosmic ray intensity changes at V1. The distance to the
 149 HP and the source spectrum are important in this calculation.

150 For the LIS Helium spectrum we use the recent spectrum of Webber and Higbie, 2009.
 151 This spectrum can be approximated to an accuracy \sim few % for energies above $\sim 100 \text{ MeV/nuc}$ by

$$152 \quad \text{Helium FLIS} = (0.99/T^{2.77}) / (1 + 4.14/T^{1.09} + 0.65/T^{2.79} + 0.0074/T^{4.20})$$

153 where T is in GeV/nuc . At the average energy of 200 MeV/nuc , this equation gives an input
 154 intensity of $0.98 \pm 0.05 \text{ p/m}^2 \cdot \text{sr}\cdot\text{s}\cdot\text{MeV/nuc}$ at the boundary at 120 (130) AU. The V1 intensity (at
 155 114 AU) measured at 2010.5 is 0.83 in the same units, about 15% lower than the IS intensity.
 156 The intensity at V2 at the same equivalent time (+0.21 year) is 0.70 and the intensity at the Earth
 157 ~ 0.89 year earlier is 0.380 in the same units.

158 Consider a simple heliosphere with a single boundary at 120 or 130 AU. The 1st step in
 159 this approach is to fit the measured intensity at the Earth which is 0.380 at 2009.6. For $K_2=0$ (no
 160 radial dependence of K) this requires values of $K_1 = 150$ (165), respectively, for the two
 161 boundary locations. These values for K_1 correspond, for each boundary location, to a
 162 modulation potential = 265 MV in the equivalent force field approximation where the
 163 modulation potential is defined as

$$\phi = \int_1^{R_B} \frac{V dr}{3K1}$$

164

165 (see Caballero-Lopez and Moraal, 2004).

166 This modulation potential is much lower than the average value of ~400-500 MV
 167 observed at previous sunspot minima in the modern era from 1950 (see e.g., Webber and Higbie
 168 2010), in keeping with the unusually high intensities observed at this time in 2009 (McDonald,
 169 Webber and Reames, 2010; Mewaldt, et al., 2010). In fact the low modulation potential that we
 170 now find (based on He nuclei) is very similar to the modulation potential obtained by Mewaldt,
 171 et al., 2010, using ACE measurements of C and Fe nuclei at the Earth at the same time in 2009.

172 For the values of K1 which fit the data at the Earth between 2005 and 2010, however, the
 173 calculated intensities at V1 and at V2 do not provide a good fit to the data lines Figure 4A in a
 174 simple 1 zone model. If the value of K is assumed to increase with r rather than be a constant,
 175 for example, $K \sim r$, the fit to the data lines in Figure 4A is still unsatisfactory. So it is clear that a
 176 simple one zone heliosphere cannot accurately determine the intensities simultaneously observed
 177 at V1, V2 and the Earth.

178 For a two zone model based on an inner heliosphere inside the HTS and an outer
 179 heliosphere (the heliosheath) between the HTS and the HP with the inner heliosphere boundary
 180 at the HTS (taken here to be at 90 AU) and the HP at 120 (130) AU, we find that, for values of
 181 the HP = 120 (130) AU, values of K1=175 (max) and 42 (min) and K2=0 with V=1.0 in the inner
 182 heliosphere and values of K1H between 18 (30) (max) and 10 (24) (min), and K2H=0 with
 183 V=0.33 in the heliosheath; the two zone model accurately fits the data at the Earth and at V1 to
 184 within $\pm 3\%$ over the entire time interval from 2004 to 2010 shown in Figure 4A.

185 As we systematically vary the values of K1 and K1H in order to fit the observed
 186 regression curves between the intensities at the Earth and V1 and the Earth and V2 during this
 187 time interval, we obtain the black and red lines shown at the time varying distances of V1 and
 188 V2 in Figure 4B. This fitting process thus provides a template as shown by these lines. This
 189 template can be moved up or down or to the left or to the right to fit the observed regression
 190 curves between the Earth data and V1 and V2 data in Figure 4A. Changes in the LIS intensity
 191 and in K1H move this template up or down and changes in K1 move it to the left or to the right.
 192 The ratio of the changes in K1 and K1H in the inner and outer heliosphere determine the slope of
 193 the black lines (these measurements are not sensitive to changes in K2). The vertical distances

194 between the V1 and V2 lines provide a continuous measure of the effective radial intensity
195 gradient between these two spacecraft.

196 These calculated intensities at the time varying distances to V1 and V2 are shown in
197 Figure 4C using a boundary at 120 AU along with the V1 and V2 data. The predictions of the
198 model give an overall average very good fit to the V1 intensity recovery during this 6 year time
199 period. The predicted V1 “line” lies an average of 2% above the data and none of the smoothed
200 data points lie more than $\pm 10\%$ from the predicted line. The passage of transient structures, the
201 largest of which occurs at 2006.15 at V2, modify the overall simple sphericity of the heliosphere.

202 For V2 the fit is less good and the calculated He intensities are an average $\sim 25\%$ less than
203 those observed, which are at times equal to those observed at V1. If the N-S asymmetry of the
204 heliosphere, which is known to be $\sim 10\%$ (see Washimi, et al., 2007; Opher, et al., 2009) is taken
205 into account, then the “effective” distance of V2 should be increased by about 10 AU and the
206 calculated intensities at V2 should be increased by $\sim 10\text{-}15\%$. This compensates for a boundary
207 shape that is squashed in the sunward direction at V2. This improves the fit between calculations
208 and data considerably as seen by the dashed line in Figure 4C, but the time periods of essentially
209 zero radial gradients between V1 and V2 in 1998-99 and 2007-2008 still require additional N-S
210 asymmetries that are time variable and mainly in the heliosheath for their explanation.

211 For a boundary at 130 AU the related fits to the data are shown in Figure 4D. The fit
212 lines are very similar to those for 120 AU but require larger K1H values and a smaller change in
213 K1H between maximum and minimum intensities than the 120 AU example. For values of the
214 boundary >130 AU the fits deteriorate rapidly for the same assumed LIS intensity

215 With regard to the diffusion coefficients used in the calculations we show in Figure 5 the
216 lower and upper limits of the values of K1 and K1H corresponding to the calculated minimum
217 intensities in 2005 and the maximum intensities in 2010. The range of values for K1 (at 1 GV)
218 from minimum to maximum intensities is from 42 to 175 and for K1H from 10 (24) -18 (30) for
219 the different HP distances of 120 (130) AU. In this case the fractional change in the diffusion
220 coefficient required to produce the minimum and maximum observed intensities in the inner
221 zone is ~ 4.2 times and the change in diffusion coefficient in the outer zone is a factor ~ 1.80
222 (1.25). These fits take into account the fact that V1 has moved outward from 94 to 115 AU
223 during the time of the measurement and V2 from 76 to 93 AU as shown by the heavy solid black
224 and red lines in Figure 4B, 4C and 4D.

225 Thus, in summary, we have the situation where (1): The magnitude of the diffusion
226 coefficient in the outer zone (heliosheath) is ~5-10 times smaller than that in the inner zone. But
227 (2): During the intensity recovery from 2005-2010 the diffusion coefficient in the inner zone
228 increases by a factor ~4.2 whereas in the outer zone this increase is only a factor ~1.80 (1.25).
229 (3): For HP distances of 130 AU or greater, the IS He intensity must increase in order to fit the
230 V1 data. (4): The observed V2 data is between 20 and 25% higher than the predictions during
231 this time period. But assuming a squashed heliosphere within an asymmetry ~10% (8-10 AU at
232 the HTS) this difference decreases to ~10% or less.

233 **Summary and Conclusions**

234 The recovery of the intensity of ~150-250 MeV/nuc cosmic ray He nuclei has been
235 followed between 2004-2010 at the Earth and also at V1 and V2 in the outer heliosphere and in
236 the case of V1, beyond the HTS. The correlation of the intensity changes at the Earth and V1 in
237 the outer heliosphere (correlation coefficient =0.922), ~100 AU apart, is remarkable after
238 accounting for a time delay ~0.9 year due to the solar wind propagation. The relative intensities
239 at V1, V2 and at the Earth as well as the slope of the regression lines between the measurements
240 place limits on the amount of solar modulation in the inner and outer heliosphere. It is found that
241 the data at the Earth and at V1 can be reproduced by a simple two zone heliosphere where the
242 intensity changes are due to changes in the cosmic ray diffusion coefficient K in each zone. In
243 the inner zone, out to the HTS assumed to be at 90 AU, the value of K is quite large (see Figure
244 5) and varies by a factor ~4.2 from the minimum to maximum modulation in this part of the solar
245 11-year cycle. In the outer zone from ~90-120 (130) AU, essentially in the heliosheath, the
246 value of the diffusion coefficient is much smaller, by a factor ~5-10 and varies by a factor ~1.80
247 (1.25) from minimum to maximum modulation.

248 Thus, in effect, because of the small value of the diffusion coefficient, the heliosheath is a
249 very turbulent, diffusive region, acting much like a diffusive barrier to these lower energy cosmic
250 rays in spite of the slower solar wind speed and other effects which tend to greatly reduce the
251 effects of adiabatic energy loss beyond the HTS.

252 Although the V1 Helium data is fit to a level $\sim\pm 5\%$ over the entire time period from
253 2004-2010 for boundaries between 120-130 AU, the V2 Helium data is not well fit with a simple
254 spherically symmetric heliosphere, with the predicted intensities typically ~25% less than the
255 data. If the heliosphere in the V2 direction is assumed to be flattened in the sunward direction

256 with an asymmetry ratio as determined by Washimi, et al., 2007, see also Opher, et al., 2009,
257 then the model fit to the V2 data is generally better (the differences between predictions and
258 observations are now ~10% or less), but the fact that there are extended periods of essentially
259 zero radial gradient between V1 and V2 require times of additional time variable asymmetries
260 between the N and S hemispheres, mainly taking place in the heliosheath.

261 The details of the fit to the data beyond the HTS depend on the values of the local
262 interstellar spectrum (LIS) used as an input to the modulation calculation and also the location of
263 the heliopause or boundary to the modulation region. For the estimated LIS He intensity used in
264 this paper the V1 data can be well fit for HP distances in the range of 120-130 AU. This
265 heliosheath region and the interstellar helium spectrum itself will be mapped in more detail as
266 V1 continues to move outward in the heliosphere and the intensity continues to increase towards
267 the LIS value.

268 **Acknowledgements:** The authors wish to thank the Voyager team (E.C. Stone, P.I.) and the
269 ACE team (R.A. Mewaldt, P.I.) for making their data available on their web-sites,
270 <http://voyager.gsfc.nasa.gov> and <http://www.srl.caltech.edu/ACE/>.

271

References

- 272
273 Caballero-Lopez, R.A. and H. Moraal (2004), Limitations of the force field equation to describe
274 cosmic ray modulation, *J. Geophys. Res.*, 109, A01101, doi:10.1029/2003JA010098
- 275 Florinski, V. and N.V. Pogorelev, (2009), Four dimensional transport of galactic cosmic rays in
276 the outer heliosphere and heliosheath, *Ap.J.*, 701, 642-651
- 277 Gleeson, L.J. and I.A. Urch, (1971), Energy losses and the modulation of galactic cosmic rays,
278 *Astrophys. Space Sci.*, 11, 288-308
- 279 Jokipii, J.R., J. Kota and Merenyi, (1993), The gradient of galactic cosmic rays at the solar wind
280 termination shock, *Ap. J.*, 405, 753-786
- 281 McDonald, F.B., W.R. Webber, E.C. Stone, A.C. Cummings, B.C. Heikkila and N. Lal, (2006),
282 Voyager observations of galactic and anomalous cosmic rays in the Heliosheath, *AIP Conf.*
283 *Proc.*, 858, 79-85, doi:10.106311.2359309
- 284 McDonald, F.B., W.R. Webber and D.V. Reames, (2010), Unusual time histories of galactic and
285 anomalous cosmic rays over the deep solar minimum of cycle 23/24, *Geophys. Res. Lett.*,
286 37, L18101, doi:10.1029/2010GL044218
- 287 Mewaldt, R.A., R. Leske and K. Lave, (2009), Cosmic ray Fe intensity reaches record levels in
288 2008-2009, *ACE News #122*, [http://www.srl.caltech.edu/ACE/ACENews/ACENews122.](http://www.srl.caltech.edu/ACE/ACENews/ACENews122.html)
289 [html](http://www.srl.caltech.edu/ACE/ACENews/ACENews122.html)
- 290 Mewaldt, R.A., et al., (2010) Record-setting cosmic ray intensities in 2009 and 2010, *Ap.J. Lett.*,
291 723, L1-L6
- 292 Opher, M., J.D. Richardson, G. Toth and T.I. Gombosi, (2009), Confronting Observations and
293 Modeling: The role of the Interstellar Magnetic Field in Voyager 1 and 2 Asymmetries,
294 *Space Sci. Rev.*, 143, 48-55
- 295 Palmer, I.D. (1982), Transport coefficient of low-energy cosmic rays in the interplanetary space,
296 *Rev. Geophys. Space Phys.*, 20, 335
- 297 Parker, E.N., (1963), *Interplanetary dynamical process*, New York, Interscience
- 298 Reinecke, J.P.L., H. Moraal and F. B. McDonald, (1993), The cosmic radiation in the
299 heliosphere at successive solar minima: Steady state no-drift solutions of the transport
300 equations, *J. Geophys. Res.*, 98, (A6), 9417-9431

- 301 Richardson, J.D., J.C. Kasper, C. Wang, J.W. Belcher and A.J. Lazarus, (2008), Cool heliosheath
302 plasma and deceleration of the upstream solar wind at the termination shock, *Nature*, 454,
303 63-66, doi:10.1038/nature07024
- 304 Washimi, H., G.R. Zank, Q. Ha, T. Tanaka and K. Munakata, (2007), A forecast of the
305 heliospheric termination shock position by three dimensional MHD stimulation, *Ap.J.*, 670,
306 L139-L142
- 307 Washimi, H., G.R. Zank, Q. Ha, T. Tanaka and K. Munakata, (2010), Realistic and time-Varying
308 Outer Heliospheric Modeling by Three-Dimensional MHD Simulation, *Ap.J.*, (in press)
- 309 Webber, W. R. and P. R. Higbie, (2009), Galactic propagation of cosmic ray nuclei in a model
310 with an increasing diffusion coefficient at low rigidities: A comparison of the new
311 interstellar spectra with Voyager data in the outer heliosphere, *J. Geophys. Res.*, 114,
312 A02103, doi:10.1029/2008JA013689.
- 313 Webber, W.R., and P.R. Higbie, (2010), What Voyager cosmic ray data in the outer heliosphere
314 tells us about ^{10}Be production in the Earths polar atmosphere in the recent past, *J. Geophys.*
315 *Res.*, 115, A05102, doi:10.1029/2009JA014512
316
317

Figure Captions

318
 319 **Figure 1:** 5 x 26-day running average of V1, V2 and IMP/ACE 150-250 MeV/nuc He nuclei
 320 data from 1998 to 2010.5. The Earth data is delayed by 0.89 year to account for inner-outer
 321 heliosphere delay in modulation due to solar wind propagation time.

322 **Figure 2:** 5 x 26 day running average of V1 to Earth ratio of 150-250 MeV/nuc He nuclei from
 323 2004 to 2010.5 (Earth data delayed by 0.89 year).

324 **Figure 3:** The V1 data from 2004.8 in Figure 1 superimposed on the data at the Earth delayed
 325 by 0.89 year (with different intensity scales on the left and right axis). This figure shows the
 326 high level of correlation between intensity changes at the Earth and in the outer heliosphere
 327 during this time period.

328 **Figure 4A:** Regression plot of the observed intensities from 2004.8 at V1 and V2 vs. the
 329 intensities at the Earth delayed by 0.89 year. Both axis in Figures 4A, 4B, 4C and 4D are
 330 $P/m^2 \cdot s \cdot sr \cdot MeV/nuc$

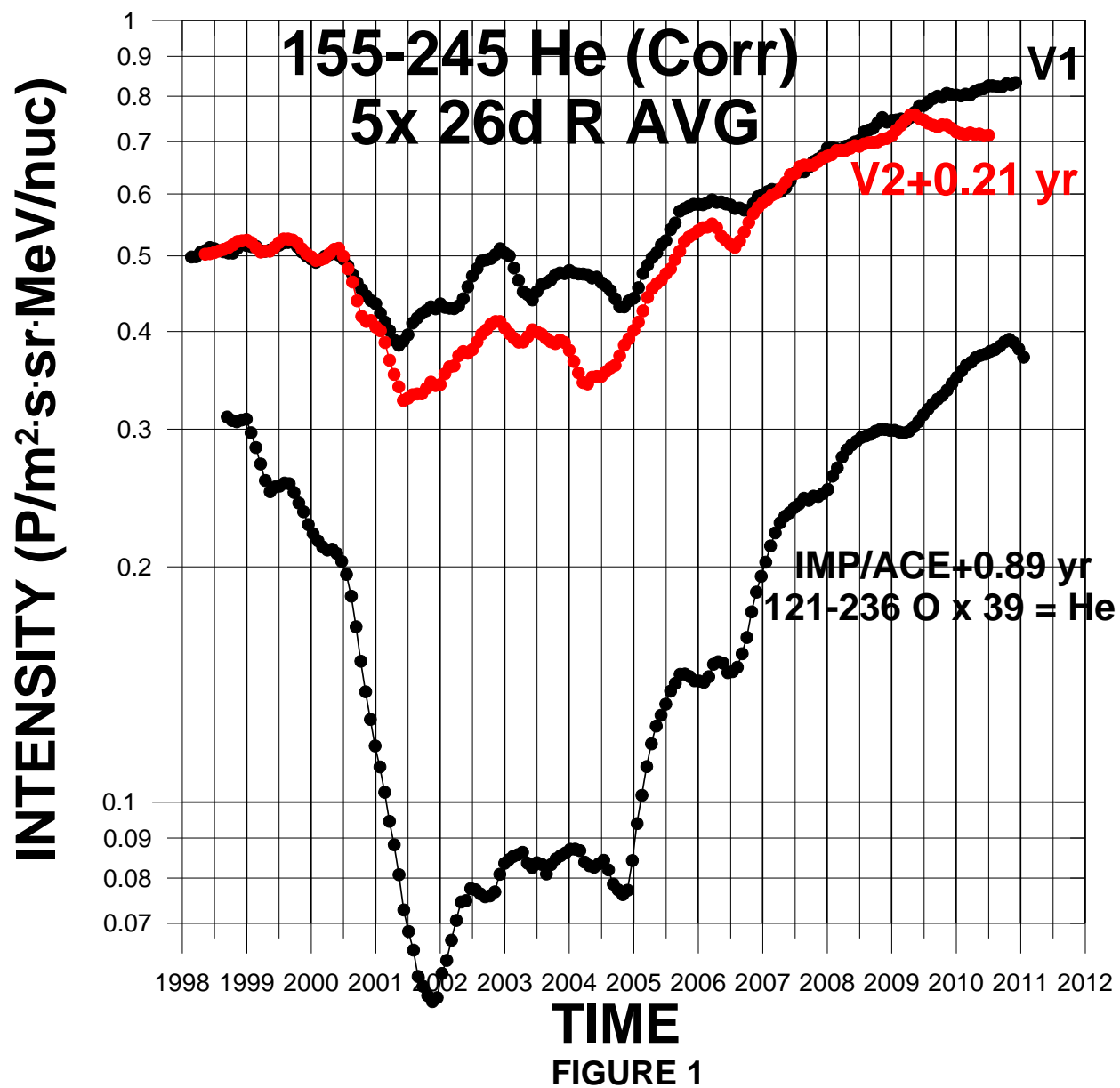
331 **Figure 4B:** Solid black (V1) and red (V2) lines show the predictions of the He nuclei intensities
 332 along the V1 and V2 trajectory in a two-zone heliospheric modulation model with the
 333 boundary at 120 AU.

334 **Figure 4C:** The V1 (black) and V2 (red) data points superimposed on the model predictions of
 335 Figure 4B, ($R_B = 120$ AU), $K1H = 18$ (max) to 10 (min). The effect of a general
 336 heliospheric radial N-S asymmetry $\sim 10\%$ near the HTS on the predictions for V2 is shown
 337 as a dashed line.

338 **Figure 4D:** Same as Figure 4C but with $R_B = 130$ AU and $K1H$ changing from 30 (max) to 24
 339 (min).

340 **Figure 5:** Values of $K1$ and $K1H$ used in the two-zone modulation model. Black lines labeled
 341 2010 and 2005 show the range of values of K in the inner heliosphere and in the heliosheath
 342 that are necessary to reproduce the He intensity changes observed between 2005 and 2010.5
 343 at the Earth and at V1 and V2. The solid points at 1 GV indicate the maximum and
 344 minimum values of $K1$ and $K1H$ at that rigidity.

345



346

347

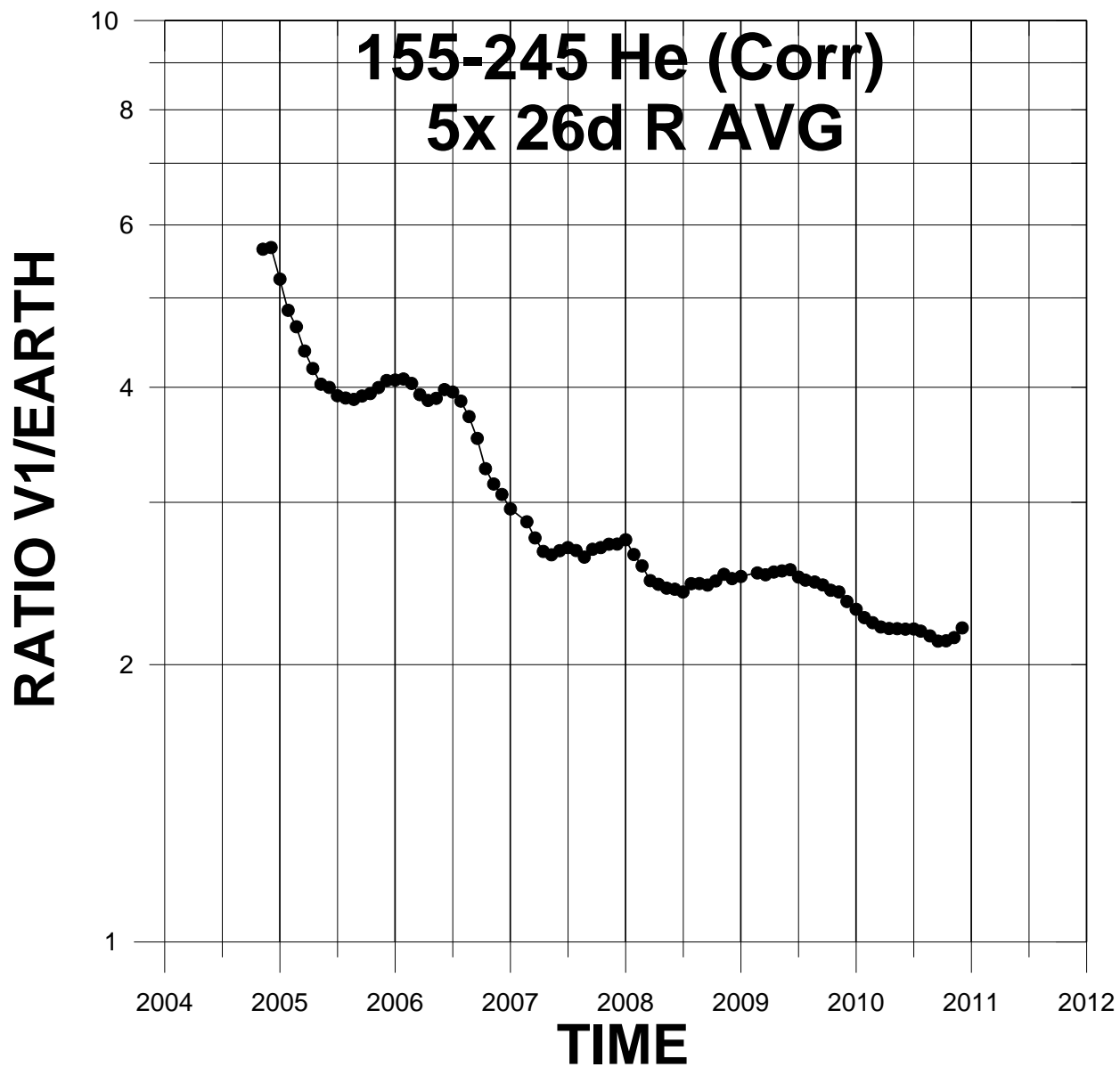


FIGURE 2

348

349

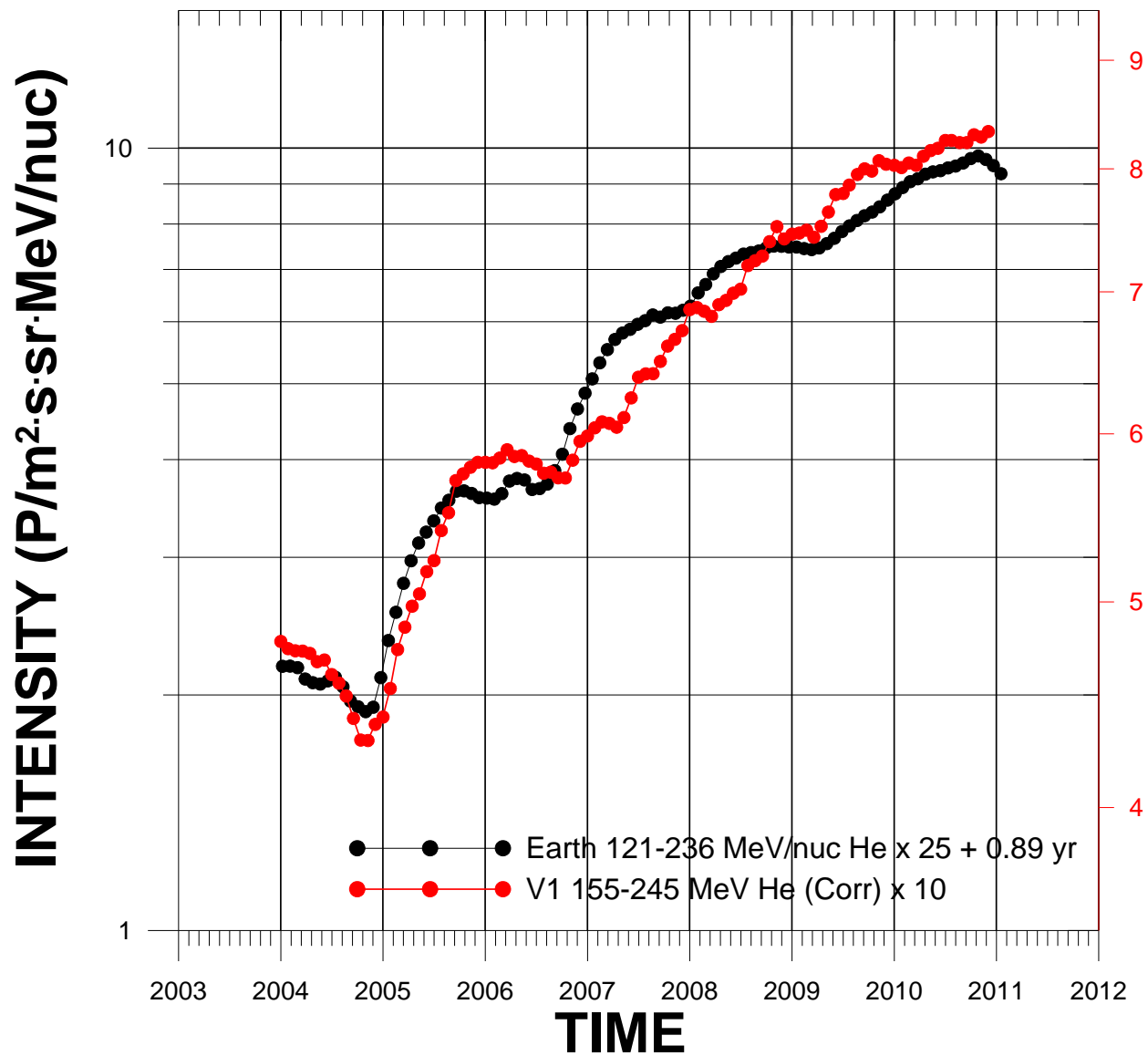
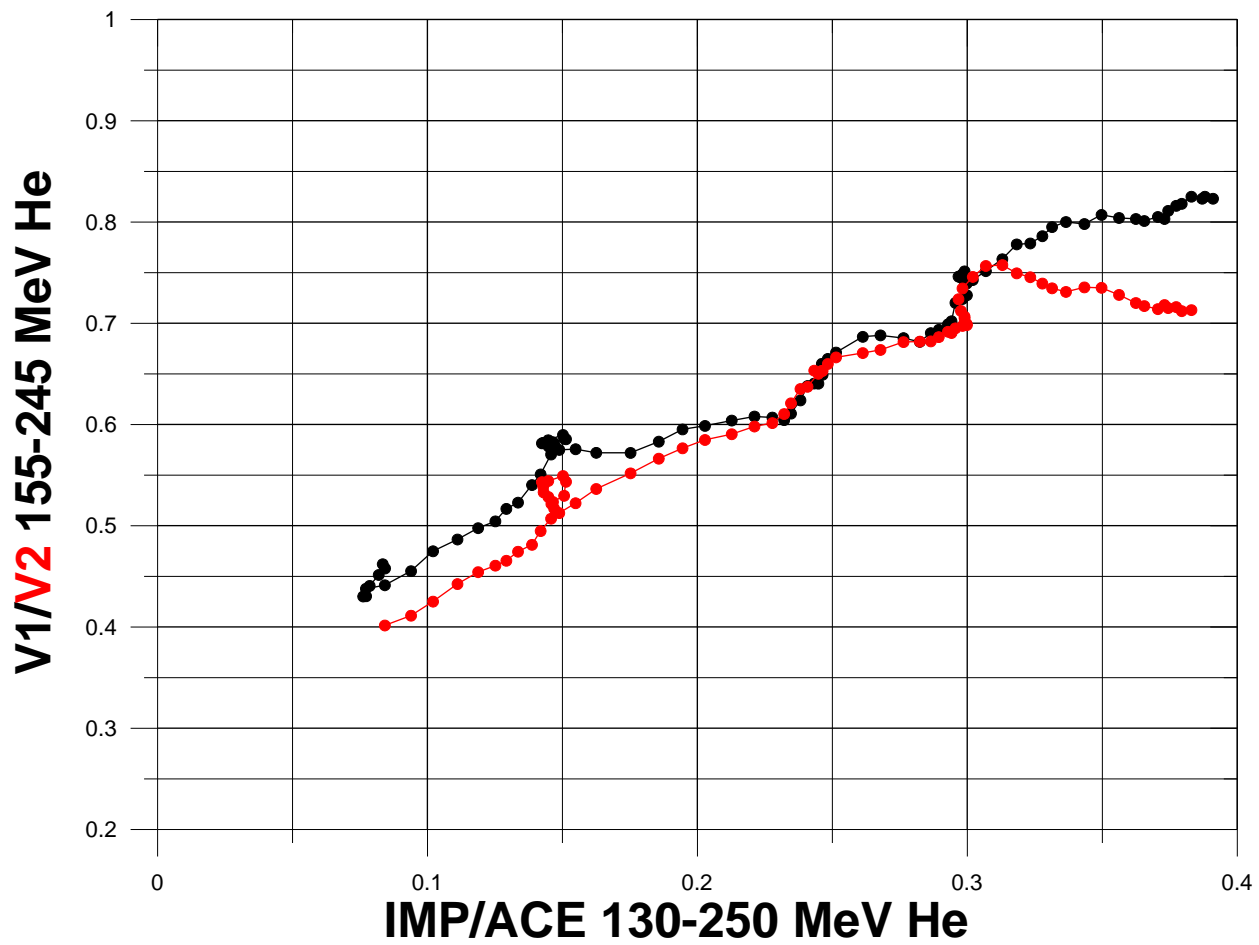


FIGURE 3

350

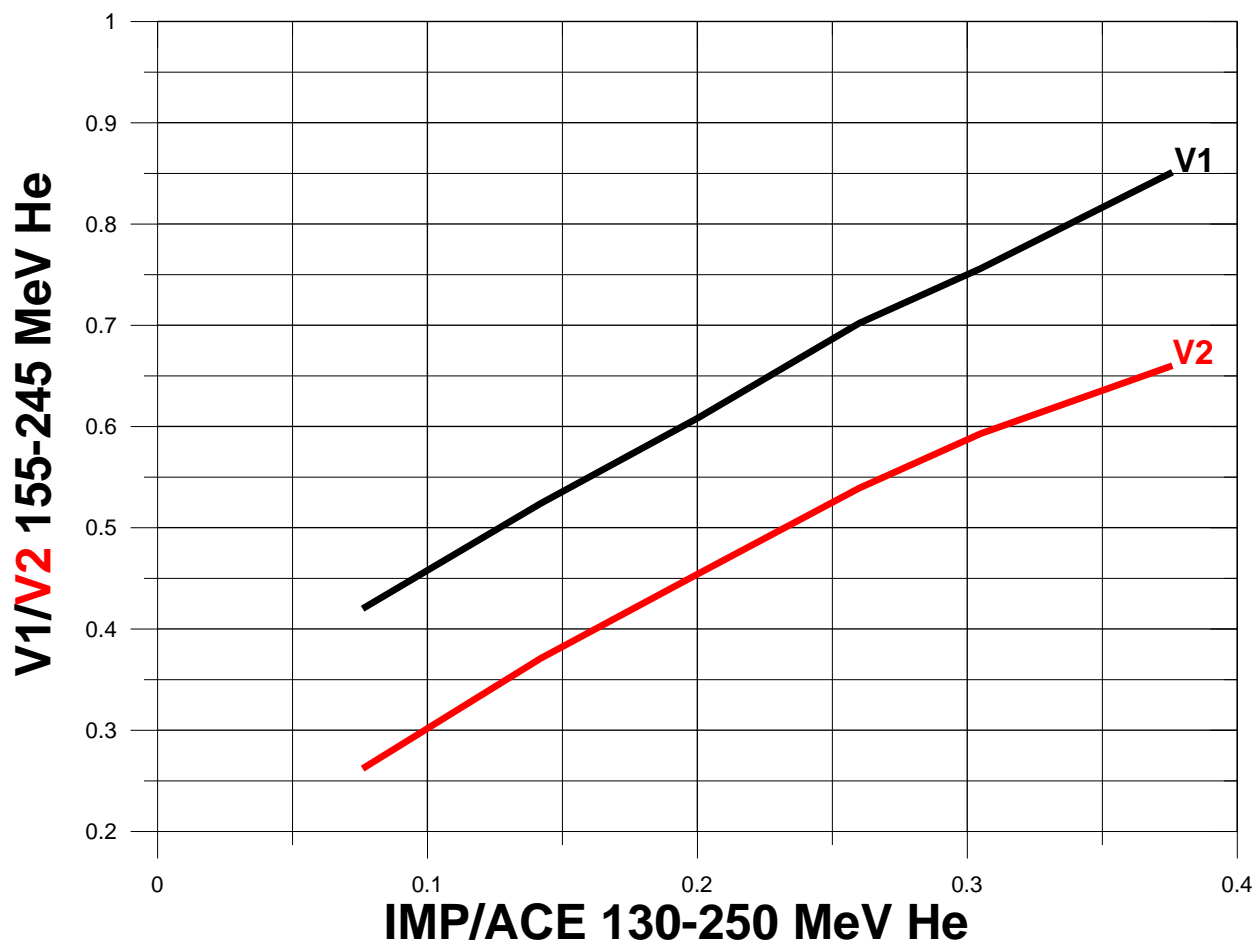
351



IMP/ACE 130-250 MeV He
FIGURE 4A

352

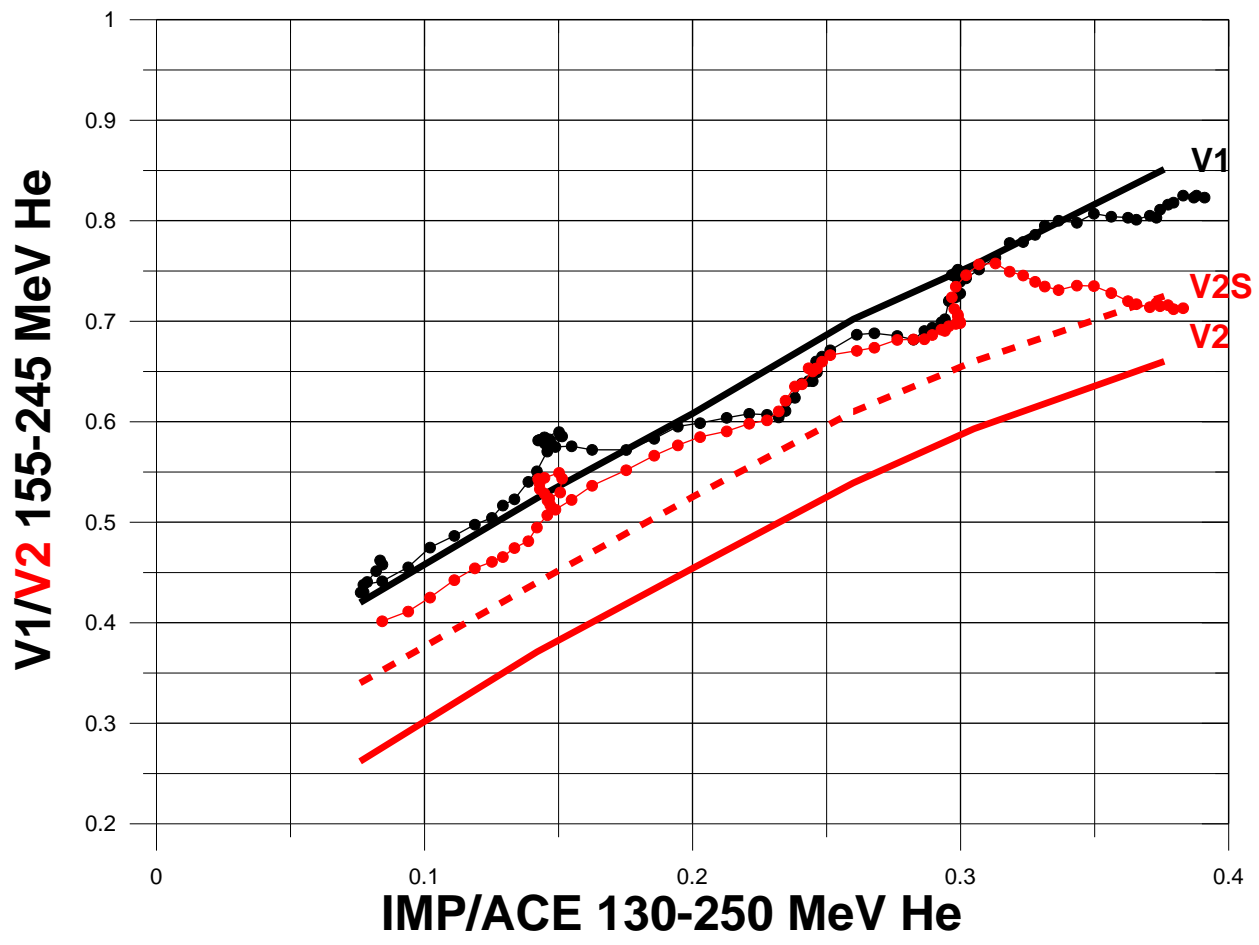
353



354

355

IMP/ACE 130-250 MeV He
FIGURE 4B



356

357

IMP/ACE 130-250 MeV He
FIGURE 4C

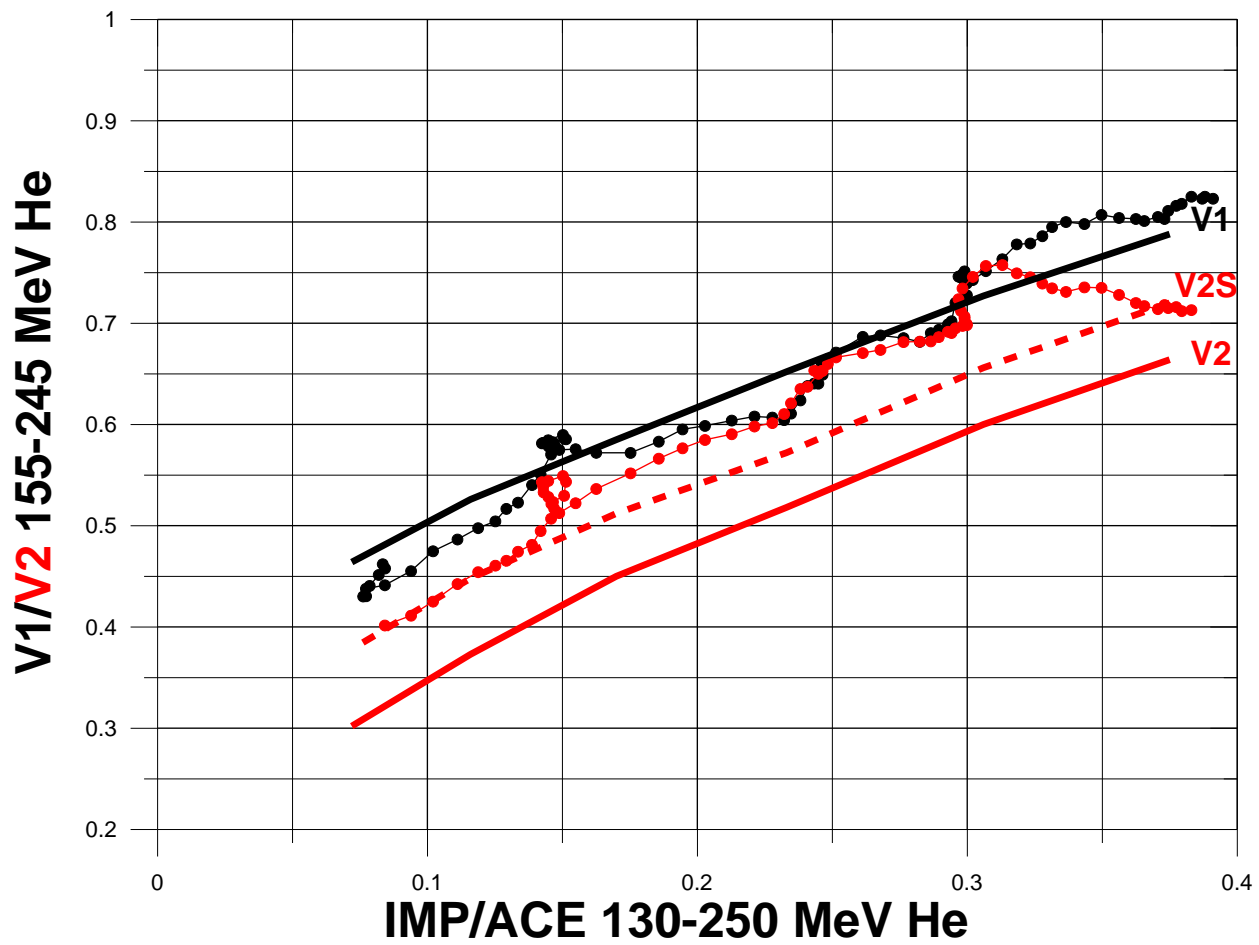
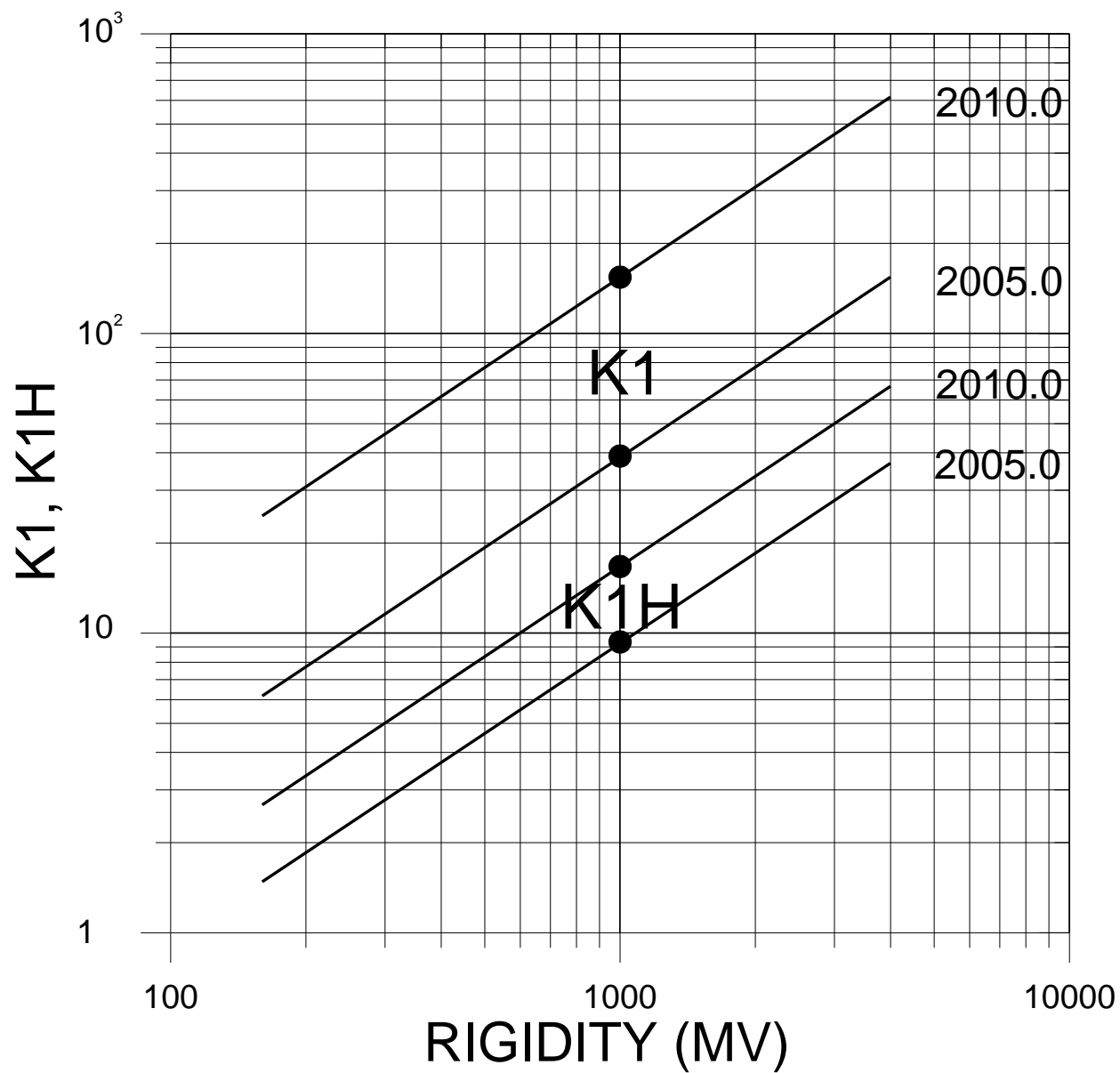


FIGURE 4D

358

359



RIGIDITY (MV)
FIGURE 5